HHS Public Access

Author manuscript

Science. Author manuscript; available in PMC 2016 March 08.

Published in final edited form as:

Science. 2016 February 26; 351(6276): 933–939. doi:10.1126/science.aad0314.

The maternal interleukin-17a pathway in mice promotes autismlike phenotypes in offspring

Gloria B. Choi[1,*], **Yeong S. Yim**[1,*], **Helen Wong**[2,3,*], **Sangdoo Kim**[4], **Hyunju Kim**[4], **Sangwon V. Kim**[5], **Charles A. Hoeffer**[2,3,†], **Dan R. Littman**[5,6,†], and **Jun R. Huh**[4,5,†]

[1]The McGovern Institute for Brain Research, Department of Brain and Cognitive Neurosciences, Massachusetts Institute of Technology, Cambridge, MA 02139, USA

[2]Center for Neural Science, New York University, New York, NY 10003, USA

[3]Institute for Behavioral Genetics, Department of Integrated Physiology, University of Colorado, Boulder, CO 80303, USA

[4]Division of Infectious Diseases and Immunology, Department of Medicine, University of Massachusetts Medical School, Worcester, MA 01605, USA

[5]The Kimmel Center for Biology and Medicine of the Skirball Institute, New York University School of Medicine, New York, NY 10016, USA

[6]Howard Hughes Medical Institute, New York, NY 10016, USA

Abstract

Viral infection during pregnancy has been correlated with increased frequency of autism spectrum disorder (ASD) in offspring. This observation has been modeled in rodents subjected to maternal immune activation (MIA). The immune cell populations critical in the MIA model have not been identified. Using both genetic mutants and blocking antibodies in mice, we show that retinoic acid receptor–related orphan nuclear receptor γt (RORγt)–dependent effector T lymphocytes [e.g., T helper 17 (T_H17) cells] and the effector cytokine interleukin-17a (IL-17a) are required in mothers for MIA-induced behavioral abnormalities in offspring. We find that MIA induces an abnormal cortical phenotype, which is also dependent on maternal IL-17a, in the fetal brain. Our data suggest that therapeutic targeting of T_H17 cells in susceptible pregnant mothers may reduce the likelihood of bearing children with inflammation-induced ASD-like phenotypes

Several studies have suggested that viral infection of women during pregnancy correlates with an increased frequency of ASD in the offspring (1–6). In the rodent maternal immune activation model of this phenomenon (7), offspring from pregnant mice infected with virus

†Corresponding author. charles.hoeffer@colorado.edu (C.A.H.); dan.littman@med.nyu.edu (D.R.L.); jun.huh@umassmed.edu (J.R.H.).

*These authors contributed equally to this work.

SUPPLEMENTARY MATERIALS

www.sciencemag.org/cgi/content/full/science.aad0314/DC1

Materials and Methods

Figs. S1 to S11

References (*45*–*47*)

or injected intra-peritoneally with synthetic dsRNA [poly(I:C)], a mimic of viral infection, exhibit behavioral symptoms reminiscent of ASD: social deficits, abnormal communication and repetitive behaviors (8). T_H17 cells are responsible for immune responses against extracellular bacteria and fungi, and their dysregulation is thought to underlie numerous inflammatory and autoimmune diseases (9), such as asthma, rheumatoid arthritis, psoriasis, inflammatory bowel disease (IBD) and multiple sclerosis. The transcription factor retinoic acid receptor–related orphan nuclear receptor gamma t (RORγt) is expressed in several cell types in the immune system. It is a key transcriptional regulator for the development of T_H17 cells, as well as γδ T cells and innate lymphoid cells (such as ILC3) that express T_H17 cell-like cytokines, in both humans and mice (10–13)

T_H17 cells and their cytokine mediators have been suggested to have a role in ASD. For example, elevated levels of IL-17a, the predominant T_H17 cytokine, have been detected in the serum of a subset of autistic children (14, 15). A genome-wide copy number variant (CNV) analysis identified *IL17A* as one of many genes enriched in autistic patients (16). Similarly, in the MIA mouse model, $CD4^+$ T lymphocytes from affected offspring produced higher levels of IL-17a upon in vitro activation (17, 18). While these data suggest that T_H17 cells may be involved in ASD patients, whether T_H17 cells are the specific immune cell population that is necessary for MIA phenotypes is unknown. Here we show that maternal RORγt-expressing pro-inflammatory T cells, a major source of IL-17a, are required in the MIA model for induction of ASD-like phenotypes in offspring. Consistent with this notion, antibody blockade of IL-17a activity in pregnant mice protected against the development of MIA-induced behavioral abnormalities in the offspring. Importantly, we also found atypical cortical development in affected offspring, and this abnormality was rescued by inhibition of maternal T_H17/IL-17a pathways.

Elevated fetal brain IL-17Ra mRNA follows increased maternal IL-17a in MIA

Pregnant mothers injected with poly(I:C) on embryonic day 12.5 (E12.5) had strong induction of serum cytokines IL-6, tumor necrosis factor-α (TNF-α), interferon-β (IFN-β) and IL-1β at 3h, compared with PBS-injected control dams (Fig. 1A and fig. S1, A to C). Additionally, poly(I:C) injection resulted in a strong increase of serum IL-17a at E14.5 (Fig. 1B). On the other hand, poly(I:C) did not affect the levels of the anti-inflammatory cytokine IL-10 in the serum nor in placenta and decidua extracts (fig. S1D). It was previously shown that the pro-inflammatory effector cytokine IL-6, a key factor for T_H17 cell differentiation (19), is required in pregnant mothers for MIA to produce ASD-like phenotypes in the offspring (7). We found that poly(I:C) injection into pregnant dams lacking IL-6 (IL-6 KO) failed to increase the serum levels of IL-17a at E14.5, consistent with IL-6 acting upstream of IL-17a. Conversely, recombinant IL-6 injections into wild-type (WT) mothers were sufficient to induce IL-17a levels comparable to those of poly(I:C)-injected WT mothers (fig. S1E). Placenta- and decidua-associated mononuclear cells, isolated from poly(I:C)-treated animals at E14.5 and cultured for 24 hours, expressed similar amounts of IL-6 mRNA compared to PBS controls (Fig. 1C). In contrast, IL-17a mRNA expression in these cells was strongly up-regulated by poly(I:C) injection (Fig. 1D). This increase in mRNA expression was correlated with enhanced secretion of IL-17a by placenta- and decidua-associated mononuclear cells from poly(I:C)-treated dams (Fig. 1E), upon ex vivo

stimulation with phorbolmyristate acetate (PMA) and ionomycin that mimics T cell receptor (TCR) activation. IL-17a induction was specific to the placenta and decidua, as small intestine mononuclear cells from poly(I:C)-treated pregnant dams did not secrete more IL-17a than those from PBS-treated controls (fig. S1F).

We also observed that expression of the IL-17a receptor subunit A (IL-17Ra), but not subunit C (IL-17Rc), mRNA was strongly augmented in the fetal brain upon induction of MIA (Fig. 1, F and G). By in situ hybridization, IL-17Ra mRNA was detected in the mouse cortex, and its expression was strongly up-regulated in E14.5 fetal brains following poly(I:C) injection of pregnant dams (Fig. 1, H and I). The in situ probe detecting endogenous expression of IL-17Ra was specific, as it did not produce detectable signal in E14.5 fetal brain that lacks IL-17Ra (fig. S2).

Maternal IL-17a promotes abnormal cortical development in offspring

We next investigated if pathological activation of the IL-17 pathway in pregnant mothers affects fetal brain development and subsequently contributes to the ASD-like behavioral phenotypes in offspring. To test this hypothesis, we pretreated pregnant mothers with isotype control or IL-17a blocking antibodies before injecting them with PBS or poly(I:C) (fig. S3). We then examined cortical development in the fetus for the following reasons: (i) Poly(I:C) injection of mothers increases IL-17Ra expression in the cortex of the fetal brain (Fig. 1, H and I); (ii) Cortical development starts approximately at E11 (20), which aligns well with the time points of potential fetal exposure to MIA (7); (iii) Disorganized cortex and focal patches of abnormal laminar cytoarchitecture have been found in the brains of ASD patients (21, 22); and (iv) MIA has been shown to affect cortical development (23, 24). We analyzed cortical lamination, an orderly layered structure of the developing cortex, in fetal brains at E14.5 and E18.5 as well as in the adult brain using antibodies specific for proteins expressed in the cortex in a layer-specific manner (25): Special AT-rich sequence-binding protein 2 (SATB2) (26), T-brain-1 (TBR1) (27), and chicken ovalbumin upstream promoter transcription factor-interacting protein 2 (CTIP2) (28). MIA led to delayed expression of SATB2 at E14.5 compared with fetuses of control animals (Fig. 2, A and C). At E18.5, MIA resulted in a patch of disorganized cortical cytoarchitecture (Fig. 2, B and D to G) but did not affect cortical thickness of the fetal brains (Fig. 2H). This singular patch of disorganized cortex occurred at a similar medial-lateral position in a majority of E18.5 fetal brains (Fig. 2, E and G) derived from mothers injected with poly(I:C), but not PBS. The abnormal expression patterns of SATB2, TBR1 and CTIP2 were maintained in adult MIA offspring (fig. S4). Importantly, normal expression of these cortical layer-specific markers, as well as laminar cortical organization, were largely preserved in the offspring of poly(I:C)-injected mothers pretreated with IL-17a blocking antibody (Fig. 2, A to D, and fig. S4).

Pretreatment with IL-17a blocking antibody also sup-pressed the MIA-mediated increase in IL-17Ra mRNA expression in fetal brain at E14.5 (Fig. 1F). This suppression was accompanied by a reduction in maternal serum IL-17a (Fig. 1B), indicating that the upregulation of IL-17Ra mRNA in fetal brains requires maternal IL-17a signaling. Of note, IL-17a antibody blockade of the IL-17a/IL-17Ra signaling pathway did not result in a concomitant increase of the serum IL-10 levels, and IL-17a mRNA expression was not

detected in fetal brain at E14.5, regardless of poly(I:C) injection. Together, these data demonstrate that the maternal IL-17a-dependent pathway mediates disorganized cortical phenotypes in offspring following *in utero* MIA and suggest that this may be due to exposure of the fetus and its brain to increased levels of IL-17a.

Maternal IL-17a promotes ASD-like behavioral abnormalities in offspring

We next tested the functional relevance of the maternal IL-17a pathway for MIA-induced ASD-like behavioral abnormalities in offspring (fig. S3). We first assessed MIA off-spring for abnormal communication by measuring pup ultrasonic vocalization (USV) responses (29). Following separation from mothers, pups from poly(I:C)-injected mothers pretreated with IgG isotype control antibody emitted more USV calls than those from PBS-injected mothers (Fig. 3A), in agreement with previous studies (29, 30). Some studies have reported reduced USV calls upon MIA (8, 31), but these opposite effects may reflect differences in methodological approaches, including dose and number of exposures to poly(I:C) as well as timing of poly(I:C) administration. Altogether, these results indicate that MIA induces abnormal USV in offspring. Pretreating poly(I:C)-injected mothers with IL-17a blocking antibody resulted in offspring that emitted a similar number of USV calls as the pups from PBS-injected control mothers (Fig. 3A), demonstrating that IL-17a-mediated signaling events are necessary for the MIA-induced abnormal USV phenotype. As previously reported (7, 8), we found that prenatal exposure to MIA also caused social interaction deficits in adult offspring (Fig. 3B). This defect was fully rescued in offspring from poly(I:C)-injected mothers pretreated with IL-17a blocking antibody (Fig. 3B). Repetitive/perseverative behaviors are another core feature in ASD that we tested next in our experimental mice using the marble burying assay (32). Offspring from poly(I:C)-injected mothers displayed enhanced marble burying com-pared with offspring from PBS-injected mothers (Fig. 3C), consistent with previous studies (7, 29). Pretreatment with IL-17a blocking antibody of poly(I:C)-injected mothers res-cued marble burying behavior in the offspring (Fig. 3C). Importantly, distinct behavioral phenotypes observed among different treatment groups were not due to differences in activity or arousal as total distances moved during the sociability or marble burying tests were indistinguishable (Fig. 3D). Moreover, different treatment groups displayed comparable gender ratios, litter sizes, and weights (fig. S5). Taken together, these data indicate that the IL-17a pathway in pregnant mice is crucial in mediating the MIA-induced behavioral phenotypes in offspring.

RORγt expression in maternal T cells is required for ASD-like phenotypes in the MIA offspring

As RORγt is a critical regulator of the IL-17a pathway (13), we next investigated the role of maternal RORγt in MIA-induced behavioral phenotypes in offspring. Importantly, T_H17 cells and IL-17a have been detected in the decidua as well as in the serum during pregnancy in humans (33–35). $CD45^+$ mononuclear cells, including $CD4^+$ T cells, isolated from placenta and decidua of immune-activated WT mothers, but not from immune-activated mothers lacking both RORγt and the closely related RORγ isoform (RORγ KO), produced IL-17a upon ex vivo activation with PMA and ionomycin (fig. S6, A and B). Cells isolated from WT and RORγ KO mice secreted similar amounts of IFN-γ, consistent with the

specific effect of RORγt on IL-17a expression (fig. S6C). In line with this observation, poly(I:C) treatment increased placenta/decidua-associated T_H17 but not regulatory T (Treg) cells in pregnant dams, compared with PBS treatment (fig. S6D and E). RORγ KO mice lack RORγ/γt expression not only in $CD4^+$ T cells, but also in other lymphoid and non-immune system cells, and they have defective development of secondary and tertiary lymphoid organs (36, 37). To determine if RORγt function specifically in T cells mediates MIA-induced phenotypes, we bred $ROR\gamma t^{FL}$ animals (fig. S7) to CD4-Cre mice to selectively inactivate *rorc(t)* in the T cells of pregnant mothers (RORγt TKO) (38). In these animals, the functions of T_H17 cells ($CD4^+ROR\gamma t^+$ cells) and other RORγt-expressing αβT cells are inhibited, but there is no effect in RORγt-expressing innate (or innate-like) immune cells, including γδT, lymphoid tissue-inducer (LTi) cells, and innate lymphoid cells type 3 (ILC3) (11, 12), as well as in RORγ-expressing non-lymphoid cells. We found that RORγt TKO mothers failed to produce IL-17a even after poly(I:C) injection (fig. S6F). Importantly, poly(I:C)-induced malformation of the cortex was prevented in offspring from RORγt TKO mothers (Fig. 4, A and B), similar to anti-IL-17a treatment (Fig. 2, B and D). Moreover, we found that prenatal expo-sure to MIA increased USV calls in pups derived from WT or RORγt HET mothers, but offspring of RORγt TKO mothers had normal USV behavior (Fig. 4C). T cell-specific deletion of maternal RORγt also abrogated the MIA-induced social interaction deficit and excessive marble burying in offspring (Fig. 4, D and E). These results were not due to general activity defects in the offspring of WT, RORγt HET, or TKO mothers (Fig. 4F). Since these offspring were derived from mating RORγt WT/HET/TKO female with WT male mice, they all carried at least one copy of functional RORγt. Therefore, the rescue of MIA-induced phenotypes observed in the offspring of RORγt TKO mothers was not likely due to the lack of T_H17 cells in the offspring. Taken together, these data indicate that maternal $CD4^+$ T lymphocytes ex-pressing RORγt (i.e., T_H17 cells) are necessary for the MIA-mediated expression of cortical abnormalities and three ASD-like behaviors modeled in mouse offspring.

IL-17a administration to the fetal brain promotes abnormal cortical development and ASD-like behavioral phenotypes

To determine if IL-17a acts on receptors in the mother or the fetus to induce the MIA phenotype, we injected poly(I:C) into IL-17Ra WT, HET or KO mothers that had been bred to IL-17Ra WT or HET males (39). Removing one or both copies of *il17ra* in the mother was sufficient to rescue the MIA-induced sociability deficit in offspring regardless of their genotypes (fig. S8A). Moreover, we found that reduced expression of maternal IL-17Ra in *il17ra* HET mothers led to reduced serum IL-17a in poly(I:C)-treated mothers (fig. S8B). Thus, it is difficult, if not impossible, to test the functional significance of the IL-17Ra in offpsring with a full germline *il17ra* KO without affecting maternal T_H17 cell activity. To circumvent this problem, we asked if increasing IL-17Ra activity in the offspring, by introducing IL-17a directly into the fetal brain in the absence of maternal inflammation, would be sufficient to induce MIA phenotypes. Injection of recombinant IL-17a protein into the ventricles of the fetal brain at E14.5 in the absence of MIA (Fig. 5A) led to the appearance of disorganized cortical patches in a similar location to those induced by MIA (Fig. 5, B to E). Unlike poly(I:C) injection, however, intra-ventricular injection of IL-17a

resulted in thinned cortical plates at the medial but not lateral part of the brain (fig. S9). This effect may reflect differences in the levels or types of inflammation associated with poly(I:C) versus IL-17a injections or the time points at which poly(I:C) (E12.5) and IL-17a (E14.5) were administered. We also found that, compared with sham injection, IL-17a injections led to an enhanced USV phenotype, social approach deficit and increased marble burying behavior, all similar in magnitude to that observed in MIA-exposed off-spring (Fig. 5, F to H). These behavioral abnormalities were not due to group differences in mobility (Fig. 5I). Importantly, neither cortical disorganization nor enhanced USV phenotypes were observed following IL-17a injections into the ventricles of IL-17Ra KO fetuses or upon IL-6 injections into WT fetal brains (fig. S10, A to C), suggesting that IL-17a, but not IL-6, acts directly in the fetal brain to induce these phenotypes. Of note, in agreement with previous reports (7, 40), IL-6 injection into pregnant WT mothers was sufficient to produce MIA-associated behavioral (enhanced USV) and cortical phenotypes in the offspring (fig. S10, D to F). Importantly, pretreatment of pregnant mothers with anti-IL-17a blocking antibody prevented the phenotypes induced by maternal IL-6 injection (fig. S10, D to F). Lastly, IL-17a injection into brains of fetuses from poly(I:C)-injected IL-6 KO mothers was sufficient to elicit increased pup USVs com-pared with PBS-injected controls (fig. S10G). These data collectively demonstrate that activation of the IL-17Ra pathway in the fetal brain, induced by intra-ventricular injection of IL-17a into the fetus or by intra-peritoneal injection of poly(I:C) or IL-6 into pregnant mothers, results in MIA-associated phenotypes in the offspring.

Therapeutic treatment with anti-IL-17a blocking anti-body in pregnant dams ameliorates MIA-associated behavioral abnormalities

Our results suggest that pathological activation of the T_H17 cell/IL-17 pathway during gestation in mothers with some inflammatory conditions may alter fetal brain development and contribute to the ASD-like behavioral phenotypes in offspring (fig. S11). T_H17 cells require RORγt for their differentiation and exert their functions by secreting multiple cytokines, including IL-17a. Abrogation of RORγt expression in maternal αβ T cells or blockade of the IL-17 pathway in pregnant dams resulted in the complete rescue of cortical developmental abnormalities and ASD-like behavioral phenotypes in offspring in the MIA rodent model. Thus, RORγt and T_H17 cells (as well as their cytokines) may serve as good therapeutic targets to prevent the development of ASD phenotypes in the children of susceptible mothers. To further test this idea, we administered anti-IL-17a antibody to pregnant mice in a time window following MIA induction (Fig. 6). We injected pregnant mothers with PBS or poly(I:C) at E12.5, followed by injection of IgG isotype control or anti-IL-17a blocking antibody at E14.5, when the delayed expression of SABT2 manifests in MIA-exposed fetal brains (Fig. 2, A and C). Compared to PBS injection followed by control anti-body treatment, poly(I:C) injection followed by anti-IL-17a antibody administration partially rescued USV and marble burying phenotypes (Fig. 6, B and D). However, MIA-induced social interaction deficits were not corrected (Fig. 6C). These effects were not due to group differences in mobility (Fig. 6E). Thus, treating pregnant mothers with anti-IL-17a after MIA can correct some of the ASD-like features, but pretreatment with anti-IL-17a antibody may have greater therapeutic potential.

Conclusions

Our results identify a specific maternal immune cell population that may have direct roles in inducing ASD-like phenotypes by acting on the developing fetal brain. These findings raise the possibility that modulation of the activity of a cytokine receptor, IL-17Ra, in the central nervous system can influence neuronal development, with implications as to specification of neuronal cell types and their connectivity. Furthermore it is worthwhile to note that the loss of certain genes that induce ASD-like phenotypes were also found with defects in cortical lamination (41, 42). These observations raise the possibility that some genetic and environmental factors that have roles in the etiology of ASD function by way of similar physiological pathways. A related question is whether IL-17Ra signaling has a normal physiological function in the fetal and adult brain, especially given the structural similarities observed between the IL-17 family cytokines and neurotrophin proteins (e.g., nerve growth factor) (43, 44). Elucidating further downstream pathways of maternal IL-17a-producing T cells, both in MIA-mothers and their offspring, will likely yield a better understanding of the mechanisms by which inflammation *in utero* contributes to the development of neurodevelopmental disorders such as ASD and may, additionally, provide insights into the roles of cytokine receptors in the central nervous system.

Supplementary Material

Refer to Web version on PubMed Central for supplementary material.

Acknowledgments

We thank E. Kurz, D. Montgomery, and Y. Cai for assistance with experiments and thank J. Koll for providing the *il17r* KO mouse line, which was originally developed by Amgen. The $il17ra^{KO}$ line will be available from D.R.L. under a material transfer agreement with Amgen. We also thank M. Sellars for critical reading of the manuscript. The data presented in this paper are tabulated in the main text and in the supplementary materials. This work was supported by the Simons Foundation Autism Research Initiative (D.R.L.), the Simons Foundation to the Simons Center for the Social Brain at MIT (Y.S.Y. and G.B.C.), Robert Buxton (G.B.C.), the National Research Foundation of Korea grants MEST-35B-2011-1-E00012 (S.K.) and NRF-2014R1A1A1006089 (H.K.), the Crohn's and Colitis Foundation of America grant 329388 (S.V.K.), the Smith Family Foundation (J.R.H.), Alzheimer's Association MNIRGDP-12-258900 (C.A.H.), NARSAD 21069 (C.A.H.), and the National Institutes of Health grants F31NS083277 (H.W.), R00DK091508 (J.R.H.), R01NS086933 (C.A.H.), and the Howard Hughes Medical Institute (D.R.L.). D.R.L. and J.R.H. are inventors on a patent application filed by New York University, related to the studies reported here

REFERENCES AND NOTES

1. Atladóttir HO, Thorsen P, Østergaard L, Schendel DE, Lemcke S, Abdallah M, Parner ET. Maternal infection requiring hospitalization during pregnancy and autism spectrum disorders. J Autism Dev. Disord. 2010; 40:1423–1430. [PubMed: 20414802]
2. Patterson PH. Immune involvement in schizophrenia and autism: Etiology, pathology and animal models. Behav. Brain Res. 2009; 204:313–321. [PubMed: 19136031]
3. Brown AS, Sourander A, Hinkka-Yli-Salomäki S, McKeague IW, Sundvall J, Surcel HM. Elevated maternal C-reactive protein and autism in a national birth cohort. Mol. Psychiatry. 2014; 19:259–264. [PubMed: 23337946]
4. Atladóttir HO, Pedersen MG, Thorsen P, Mortensen PB, Deleuran B, Eaton WW, Parner ET. Association of family history of autoimmune diseases and autism spectrum disorders. Pediatrics. 2009; 124:687–694. [PubMed: 19581261]

5. Ashwood P, Wills S, Van de Water J. The immune response in autism: A new frontier for autism research. J Leukoc. Biol. 2006; 80:1–15. [PubMed: 16698940]
6. Lee BK, Magnusson C, Gardner RM, Blomström Å, Newschaffer CJ, Burstyn I, Karlsson H, Dalman C. Maternal hospitalization with infection during pregnancy and risk of autism spectrum disorders. Brain Behav. Immun. 2015; 44:100–105. [PubMed: 25218900]
7. Smith SEP, Li J, Garbett K, Mirnics K, Patterson PH. Maternal immune activation alters fetal brain development through interleukin-6. J Neurosci. 2007; 27:10695–10702. [PubMed: 17913903]
8. Malkova NV, Yu CZ, Hsiao EY, Moore MJ, Patterson PH. Maternal immune activation yields offspring displaying mouse versions of the three core symptoms of autism. Brain Behav. Immun. 2012; 26:607–616. [PubMed: 22310922]
9. Wilke CM, Bishop K, Fox D, Zou W. Deciphering the role of T_h17 cells in human disease. Trends Immunol. 2011; 32:603–611. [PubMed: 21958759]
10. Manel N, Unutmaz D, Littman DR. The differentiation of human T_H-17 cells requires transforming growth factor-beta and induction of the nuclear receptor RORgammat. Nat. Immunol. 2008; 9:641–649. [PubMed: 18454151]
11. Spits H, Di Santo JP. The expanding family of innate lymphoid cells: Regulators and effectors of immunity and tissue remodeling. Nat. Immunol. 2011; 12:21–27. [PubMed: 21113163]
12. Lochner M, Peduto L, Cherrier M, Sawa S, Langa F, Varona R, Riethmacher D, Si-Tahar M, Di Santo JP, Eberl G. In vivo equilibrium of proinflammatory IL-17+ and regulatory IL-10+ Foxp3+ RORgamma t+ T cells. J Exp. Med. 2008; 205:1381–1393. [PubMed: 18504307]
13. Ivanov II, McKenzie BS, Zhou L, Tadokoro CE, Lepelley A, Lafaille JJ, Cua DJ, Littman DR. The orphan nuclear receptor RORgammat directs the differentiation program of proinflammatory IL-17+ T helper cells. Cell. 2006; 126:1121–1133. [PubMed: 16990136]
14. Al-Ayadhi LY, Mostafa GA. Elevated serum levels of interleukin-17A in children with autism. J Neuroinflammation. 2012; 9:158. [PubMed: 22748016]
15. Suzuki K, Matsuzaki H, Iwata K, Kameno Y, Shimmura C, Kawai S, Yoshihara Y, Wakuda T, Takebayashi K, Takagai S, Matsumoto K, Tsuchiya KJ, Iwata Y, Nakamura K, Tsujii M, Sugiyama T, Mori N. Plasma cytokine profiles in subjects with high-functioning autism spectrum disorders. PLOS ONE. 2011; 6:e20470. [PubMed: 21647375]
16. van der Zwaag B, Franke L, Poot M, Hochstenbach R, Spierenburg HA, Vorstman JA, van Daalen E, de Jonge MV, Verbeek NE, Brilstra EH, van 't Slot R, Ophoff RA, van Es MA, Blauw HM, Veldink JH, Buizer-Voskamp JE, Beemer FA, van den Berg LH, Wijmenga C, van Amstel HK, van Engeland H, Burbach JP, Staal WG. Gene-network analysis identifies susceptibility genes related to glycobiology in autism. PLOS ONE. 2009; 4:e5324. [PubMed: 19492091]
17. Mandal M, Marzouk AC, Donnelly R, Ponzio NM. Preferential development of Th17 cells in offspring of immunostimulated pregnant mice. J Reprod. Immunol. 2010; 87:97–100. [PubMed: 20727596]
18. Hsiao EY, McBride SW, Chow J, Mazmanian SK, Patterson PH. Modeling an autism risk factor in mice leads to permanent immune dysregulation. Proc. Natl. Acad. Sci. U.S.A. 2012; 109:12776–12781. [PubMed: 22802640]
19. Kuchroo VK, Awasthi A. Emerging new roles of T_h17 cells. Eur. J. Immunol. 2012; 42:2211–2214. [PubMed: 22949318]
20. Dehay C, Kennedy H. Cell-cycle control and cortical development. Nat. Rev. Neurosci. 2007; 8:438–450. [PubMed: 17514197]
21. Casanova MF, El-Baz AS, Kamat SS, Dombroski BA, Khalifa F, Elnakib A, Soliman A, Allison-McNutt A, Switala AE. Focal cortical dysplasias in autism spectrum disorders. Acta Neuropathol. Commun. 2013; 1:67. [PubMed: 24252498]
22. Stoner R, Chow ML, Boyle MP, Sunkin SM, Mouton PR, Roy S, Wynshaw-Boris A, Colamarino SA, Lein ES, Courchesne E. Patches of disorganization in the neocortex of children with autism. N Engl. J. Med. 2014; 370:1209–1219. [PubMed: 24670167]
23. De Miranda J, Yaddanapudi K, Hornig M, Villar G, Serge R, Lipkin WI. Induction of Toll-like receptor 3-mediated immunity during gestation inhibits cortical neurogenesis and causes behavioral disturbances. MBio. 2010; 1:e00176-10–e00176-19. [PubMed: 20941330]

24. Smith SE, Elliott RM, Anderson MP. Maternal immune activation increases neonatal mouse cortex thickness and cell density. J Neuroimmune Pharmacol. 2012; 7:529–532. [PubMed: 22570011]
25. Molyneaux BJ, Arlotta P, Menezes JR, Macklis JD. Neuronal subtype specification in the cerebral cortex. Nat. Rev. Neurosci. 2007; 8:427–437. [PubMed: 17514196]
26. Alcamo EA, Chirivella L, Dautzenberg M, Dobreva G, Fariñas I, Grosschedl R, McConnell SK. Satb2 regulates callosal projection neuron identity in the developing cerebral cortex. Neuron. 2008; 57:364–377. [PubMed: 18255030]
27. Englund C, Fink A, Lau C, Pham D, Daza RA, Bulfone A, Kowalczyk T, Hevner RF. Pax6, Tbr2, and Tbr1 are expressed sequentially by radial glia, intermediate progenitor cells, and postmitotic neurons in developing neocortex. J Neurosci. 2005; 25:247–251. [PubMed: 15634788]
28. Leid M, Ishmael JE, Avram D, Shepherd D, Fraulob V, Dollé P. CTIP1 and CTIP2 are differentially expressed during mouse embryogenesis. Gene Expr. Patterns. 2004; 4:733–739. [PubMed: 15465497]
29. Schwartzer JJ, Careaga M, Onore CE, Rushakoff JA, Berman RF, Ashwood P. Maternal immune activation and strain specific interactions in the development of autism-like behaviors in mice. Transl. Psychiatry. 2013; 3:e240. [PubMed: 23481627]
30. Yee N, Schwarting RK, Fuchs E, Wöhr M. Increased affective ultrasonic communication during fear learning in adult male rats exposed to maternal immune activation. J Psychiatr. Res. 2012; 46:1199–1205. [PubMed: 22687817]
31. Hsiao EY, McBride SW, Hsien S, Sharon G, Hyde ER, McCue T, Codelli JA, Chow J, Reisman SE, Petrosino JF, Patterson PH, Mazmanian SK. Microbiota modulate behavioral and physiological abnormalities associated with neurodevelopmental disorders. Cell. 2013; 155:1451–1463. [PubMed: 24315484]
32. Hoeffer CA, Tang W, Wong H, Santillan A, Patterson RJ, Martinez LA, Tejada-Simon MV, Paylor R, Hamilton SL, Klann E. Removal of FKBP12 enhances mTOR-Raptor interactions, LTP, memory, and perseverative/repetitive behavior. Neuron. 2008; 60:832–845. [PubMed: 19081378]
33. Wu HX, Jin LP, Xu B, Liang SS, Li DJ. Decidual stromal cells recruit T_h17 cells into decidua to promote proliferation and invasion of human trophoblast cells by secreting IL-17. Cell. Mol. Immunol. 2014; 11:253–262. [PubMed: 24633013]
34. Nakashima A, Ito M, Yoneda S, Shiozaki A, Hidaka T, Saito S. Circulating and decidual Th17 cell levels in healthy pregnancy. Am. J. Reprod. Immunol. 2010; 63:104–109. [PubMed: 20015328]
35. Martínez-García EA, Chávez-Robles B, Sánchez-Hernández PE, Núñez-Atahualpa L, Martín-Máquez BT, Muñoz-Gómez A, González-López L, Gámez-Nava JI, Salazar-Páramo M, Dávalos-Rodríguez I, Petri MH, Zúñiga-Tamayo D, Vargas-Ramírez R, Vázquez-Del Mercado M. IL-17 increased in the third trimester in healthy women with term labor. Am. J. Reprod. Immunol. 2011; 65:99–103. [PubMed: 20618180]
36. Eberl G, Littman DR. Thymic origin of intestinal alphabeta T cells revealed by fate mapping of RORgammat+ cells. Science. 2004; 305:248–251. [PubMed: 15247480]
37. Sun Z, Unutmaz D, Zou YR, Sunshine MJ, Pierani A, Brenner-Morton S, Mebius RE, Littman DR. Requirement for RORgamma in thymocyte survival and lymphoid organ development. Science. 2000; 288:2369–2373. [PubMed: 10875923]
38. Huh JR, Leung MW, Huang P, Ryan DA, Krout MR, Malapaka RR, Chow J, Manel N, Ciofani M, Kim SV, Cuesta A, Santori FR, Lafaille JJ, Xu HE, Gin DY, Rastinejad F, Littman DR. Digoxin and its derivatives suppress T_H17 cell differentiation by antagonizing RORγt activity. Nature. 2011; 472:486–490. [PubMed: 21441909]
39. Iwakura Y, Ishigame H, Saijo S, Nakae S. Functional specialization of interleukin-17 family members. Immunity. 2011; 34:149–162. [PubMed: 21349428]
40. Hsiao EY, Patterson PH. Activation of the maternal immune system induces endocrine changes in the placenta via IL-6. Brain Behav. Immun. 2011; 25:604–615. [PubMed: 21195166]
41. Orosco LA, Ross AP, Cates SL, Scott SE, Wu D, Sohn J, Pleasure D, Pleasure SJ, Adamopoulos IE, Zarbalis KS. Loss of Wdfy3 in mice alters cerebral cortical neurogenesis reflecting aspects of the autism pathology. Nat. Commun. 2014; 5:4692. [PubMed: 25198012]
42. Peñagarikano O, Abrahams BS, Herman EI, Winden KD, Gdalyahu A, Dong H, Sonnenblick LI, Gruver R, Almajano J, Bragin A, Golshani P, Trachtenberg JT, Peles E, Geschwind DH. Absence

of CNTNAP2 leads to epilepsy, neuronal migration abnormalities, and core autism-related deficits. Cell. 2011; 147:235–246. [PubMed: 21962519]

43. Hymowitz SG, Filvaroff EH, Yin JP, Lee J, Cai L, Risser P, Maruoka M, Mao W, Foster J, Kelley RF, Pan G, Gurney AL, de Vos AM, Starovasnik MA. IL-17s adopt a cystine knot fold: Structure and activity of a novel cytokine, IL-17F, and implications for receptor binding. EMBO J. 2001; 20:5332–5341. [PubMed: 11574464]
44. Zhang X, Angkasekwinai P, Dong C, Tang H. Structure and function of interleukin-17 family cytokines. Protein Cell. 2011; 2:26–40. [PubMed: 21337007]
45. Chen K, McAleer JP, Lin Y, Paterson DL, Zheng M, Alcorn JF, Weaver CT, Kolls JK. T_h17 cells mediate clade-specific, serotype-independent mucosal immunity. Immunity. 2011; 35:997–1009. [PubMed: 22195749]
46. Ivanov II, Atarashi K, Manel N, Brodie EL, Shima T, Karaoz U, Wei D, Goldfarb KC, Santee CA, Lynch SV, Tanoue T, Imaoka A, Itoh K, Takeda K, Umesaki Y, Honda K, Littman DR. Induction of intestinal T_h17 cells by segmented filamentous bacteria. Cell. 2009; 139:485–498. [PubMed: 19836068]
47. Hoeffer CA, Wong H, Cain P, Levenga J, Cowansage KK, Choi Y, Davy C, Majmundar N, McMillan DR, Rothermel BA, Klann E. Regulator of calcineurin 1 modulates expression of innate anxiety and anxiogenic responses to selective serotonin reuptake inhibitor treatment. J Neurosci. 2013; 33:16930–16944. [PubMed: 24155299]

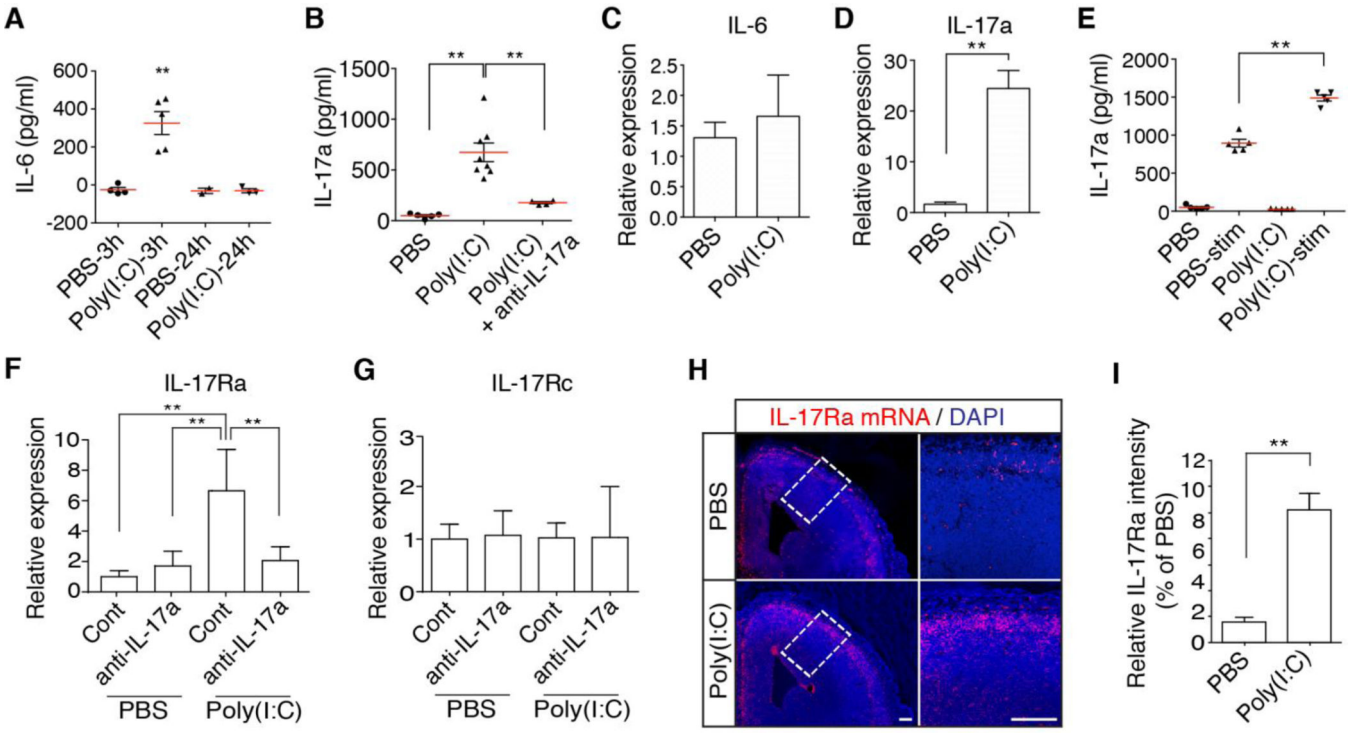

Fig. 1. IL-17a increase in mothers subjected to MIA leads to elevated IL-17Ra mRNA expression in the offspring

(**A**) Serum concentrations of IL-6 (*n* = 3–5 mice per group, 2 independent experiments) at 3 or 24 hours after PBS or poly(I:C) injection into pregnant dams at E12.5. (**B**) Serum concentrations of maternal IL-17a (*n* = 4–8 mice per group, 2 independent experiments) at E14.5 in PBS- or poly(I:C)-injected mothers, pretreated with or without IL-17a blocking antibodies. (**C** and **D**) Relative IL-6 (C) and IL-17a (D) mRNA expression in cells isolated from placenta/decidua of PBS- or poly(I:C)-treated mothers at E14.5 and cultured in vitro for 24 hours,. The results are representative of three independent experiments. For each probe set, relative mRNA expression of one biological replicate from PBS-treated dams was set at 1. Real-time PCR analysis of relative expression of indicated genes compared to the level of Gapdh in cells from PBS-treated dams. (**E**) Supernatant concentrations of IL-17a from ex vivo cultured mononuclear cells, isolated from placenta/decidua of PBS- or poly(I:C)-treated pregnant dams. Stim refers to PMA and lonomycin stimulation. (**F** and **G**) Relative IL-17Ra (F) and IL-17Rc (G) mRNA levels in E14.5 male fetal brain, derived from PBS- or Poly(I:C)-injected mothers, pretreated with isotype control (Cont) or IL-17a blocking antibodies (anti-IL-17a). The relative mRNA fold change, compared to the PBS and Cont-treated group, is plotted on the y-axis (*n* = 7 (PBS, Cont), *n* = 7 (PBS, anti-IL-17a), *n* = 7 (Poly(I:C), Cont), *n* = 7 (Poly(I:C), anti-IL-17a); from 2–3 independent experiments). (**H**) In situ hybridization with an IL-17Ra RNA probe in E14.5 male fetal brains derived from PBS- or poly(I:C)- injected mothers. Images are representative of four independent experiments. (**I**) Relative signal intensity for images shown in (H). Scale bar represents 100 μm. (A, B, E, F and G) One-way ANOVA with Tukey post-hoc tests. (C, D and I) Student's *t* test. $^{**}P < 0.01$. Graphs show mean ± SEM.

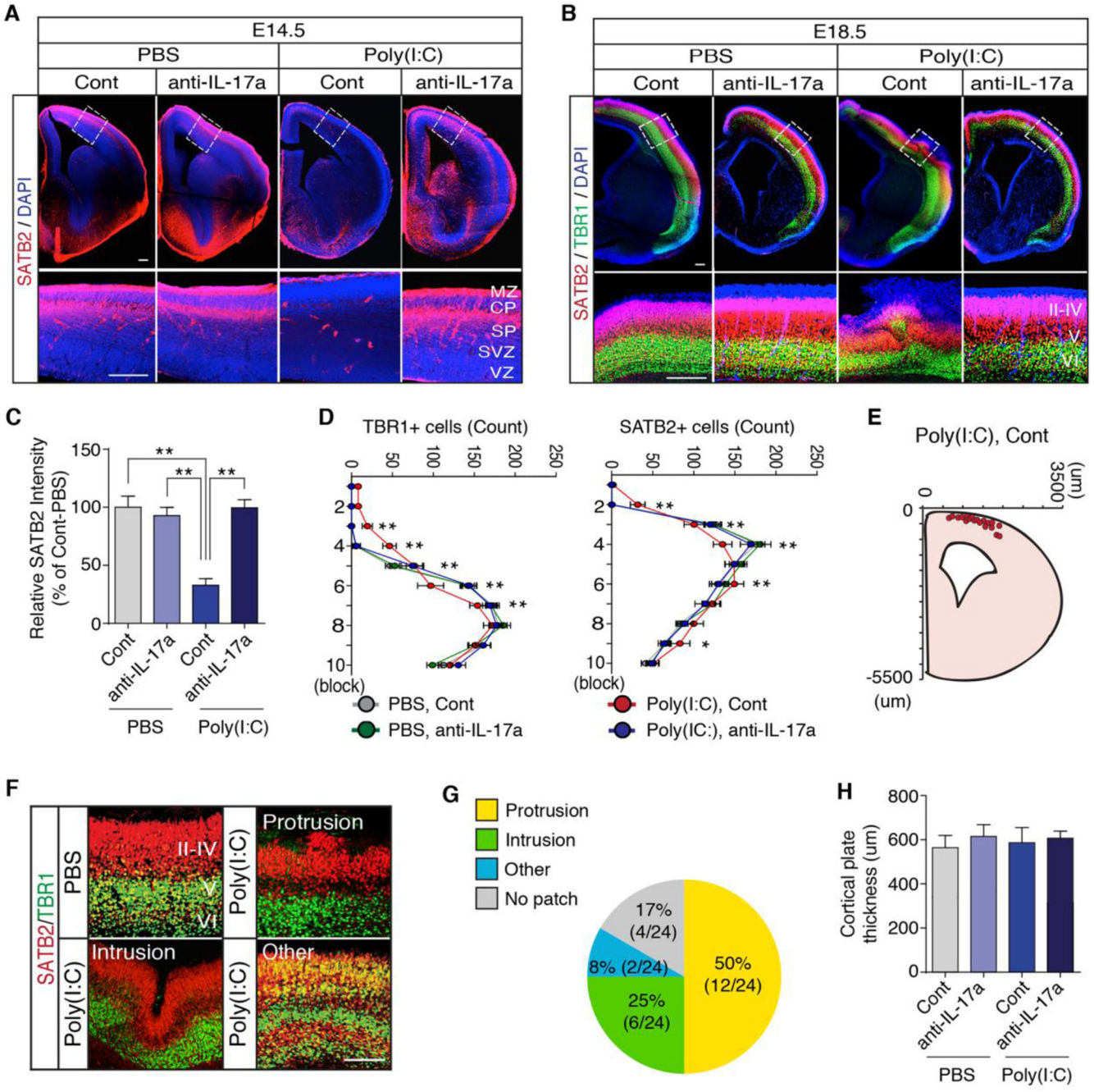

Fig. 2. The IL-17a pathway promotes abnormal cortical development in the offspring of pregnant dams following MIA

(**A**) Immuno-fluorescence staining of SATB2 (a marker of postmitotic neurons in superficial cortical layers) in E14.5 male fetal brain, derived from PBS- or poly(I:C)-injected mothers, pretreated with isotype control (Cont) or IL-17a blocking antibodies (anti-IL-17a). (MZ: marginal zone, CP: cortical plate, SP: subplate, SVZ: subventricular zone, VZ: ventricular zone). (**B**) Staining of SATB2 and TBR1 (a marker restricted to deeper cortical layers) in E18.5 male fetal brains from animals treated as in (A). II–IV, V and VI refer to different cortical layers. (**C**) Quantification of SATB2 intensity in the cortical plate of E14.5 fetal

brains (*n* = 8 (PBS, Cont), *n* = 8 (PBS, anti-IL-17a), *n* = 8 (Poly(l:C), Cont), *n* = 8 (Poly(l:C), anti-IL-17a), 3 independent experiments). (**D**) Quantification of TBR1 and SATB2 positive cells in a 300×300 μm^2 region of interest (ROI) centered on the malformation in the cortical plate of E18.5 fetal brains (*n* = 20 (PBS, Cont), *n* = 20 (PBS, anti-IL-17a), *n* = 24 (Poly(l:C), Cont), *n* = 20 (Poly(l:C), anti-IL-17a), 5 independent experiments). (**E**) The spatial location of the cortical patch in E18.5 male fetal brains from poly(l:C)-injected mothers pretreated with control antibodies (*n* = 20 (Poly(l:C),Cont)). (**F**) The disorganized patches of cortex observed in fetuses from poly(l:C)-injected mothers were categorized into groups based on morphology: Protrusions, intrusions or other abnormal patterns and their representative images are shown. (**G**) Percentage of the cortical patches in each category (*n* = 24 (Poly(l:C), Cont)). (**H**) Thickness of the cortical plate in E18.5 fetal brains, derived from PBS- or poly(l:C)-injected mothers, pretreated with isotype control or IL-17a blocking antibodies (*n* = 20 (PBS, Cont), *n* = 20 (PBS, anti-IL-17a), *n* = 20 (Poly(l:C), Cont), *n* = 20 (Poly(l:C), anti-IL-17a), 5 independent experiments). (A, B and F) Scale bar represents 100 μm. One-way ANOVA (C and H) and Two-way ANOVA (D) with Tukey post-hoc tests. $^{**}P < 0.01$ and $^{*}P < 0.05$. Graphs show mean ± SEM.

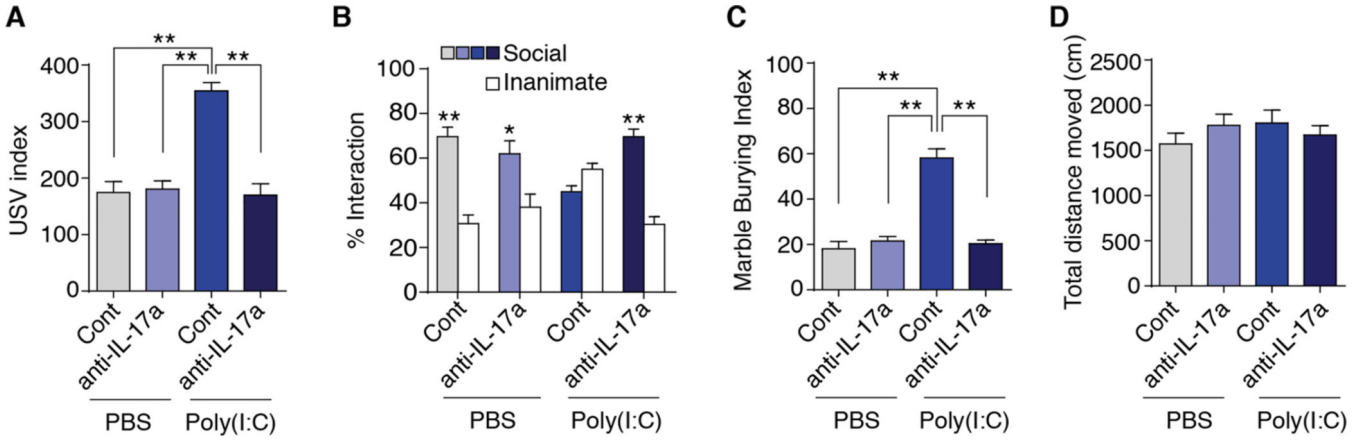

Fig. 3. The IL-17a pathway promotes ASD-like phenotypes in the MIA offspring

(**A**) Ultrasonic vocalization (USV) assay. At P9, pups from the indicated experimental groups were separated from their mothers to elicit USV calls. The number of pup calls is plotted on the y-axis (n = 25 (PBS, Cont), n = 28 (PBS, anti-IL-17a), n = 38 (Poly(I:C), Cont), n = 34 (Poly(I:C), anti-IL-17a); from 6–7 independent experiments. (**B**) Social approach behavior. Graphed as a social preference index (% time spent investigating social or inanimate stimulus out of total object investigation time) (n = 15 (PBS, Cont), n = 15 (PBS, anti-IL-17a), n = 16 (Poly(I:C), Cont), n = 20 (Poly(I:C), anti-IL-17a); from 6–7 independent experiments. (**C**) Marble burying behavior. Percentage of the number of buried marbles is plotted on the y-axis (n = 15 (PBS, Cont), n = 15 (PBS, anti-IL-17a), n = 15 (Poly(I:C), Cont), n = 20 (Poly(I:C), anti-IL-17a); from 6–7 independent experiments. (**D**) Total distance traveled during social approach behavior. (A, C and D) One-way ANOVA with Tukey post-hoc tests. (B) Two-way ANOVA with Tukey post-hoc tests. $^{**}P < 0.01$ and $^{*}P < 0.05$. Graphs show mean ± SEM.

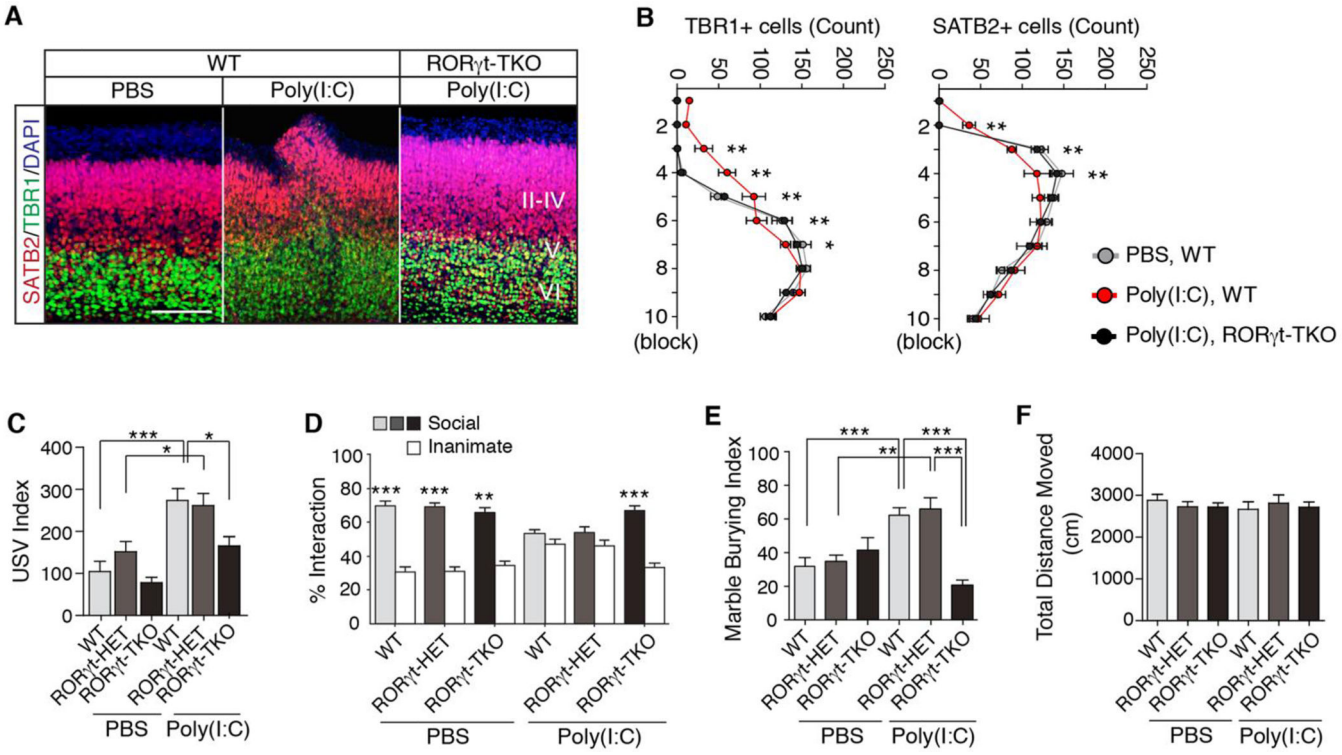

Fig. 4. RORγt expression in maternal T cells is required for manifestation of ASD-like phenotypes in the MIA model

(**A**) SATB2 and TBR1 staining in the cortex of E18.5 fetal brains following MIA induction with poly(I:C) in mothers with the indicated genotypes. II–IV, V and VI refer to different cortical layers. Images are representative of three independent experiments. Scale bar represents 100 μm. (**B**) Quantification of TBR1 and SATB2 positive cells in a 300×300 μm^2 ROI centered on the malformation in the cortical plate of E18.5 male fetal brains (n = 6 (PBS, WT), n = 6 (Poly(I:C), WT), n = 6 (Poly(I:C), RORγt-TKO)). (**C**) Number of ultrasonic vocalizations (USV)s emitted by P9 pups. Total USVs emitted during test period (3 min) are plotted on the y-axis (n = 16,18 and 15 offspring from PBS-treated WT, RORγt HET and RORγt TKO mothers; n = 15,11 and 28 from poly(I:C)-treated WT, RORγt HET and RORγt TKO mothers); data from 4–7 independent dams. (**D**) Social approach behavior is graphed as a social preference index (% time spent investigating social or inanimate stimulus/ total exploration time for both objects), (n = 21, 15 and 15 adult offspring from PBS-treated WT, RORγt HET and RORγt TKO mothers; n = 36,15 and 21 from poly(I:C)-treated WT, RORγt HET and RORγt TKO mothers); data from 4–7 independent dams. (**E**) Marble burying behavior is graphed as the percentage of buried marbles, (n = 14,19 and 15 adult offspring from PBS-treated WT, RORγt HET and RORγt TKO mothers; n = 32,15 and 25 from poly(I:C)-treated WT, RORγt HET and RORγt TKO mice per group); data from 4–7 independent dams. (**F**) Total distance moved by offspring tested for social behavior and marble burying. RORγt HET and RORγt TKO refer to *RORγ$^{Neo/+}$; CD4-Cre*/+ and *RORγt^{FL}/RORγ^{Neo}; CD4-Cre*/+, respectively. (**C**) One-way ANOVA with Holm-Sidak post-hoc tests. (B and D) Two-way ANOVA with Tukey post-hoc tests. (E and F) One-way

ANOVA with Tukey post-hoc tests. ***P <0.001, **P < 0.01 and *P < 0.05. Graphs show mean ± SEM.

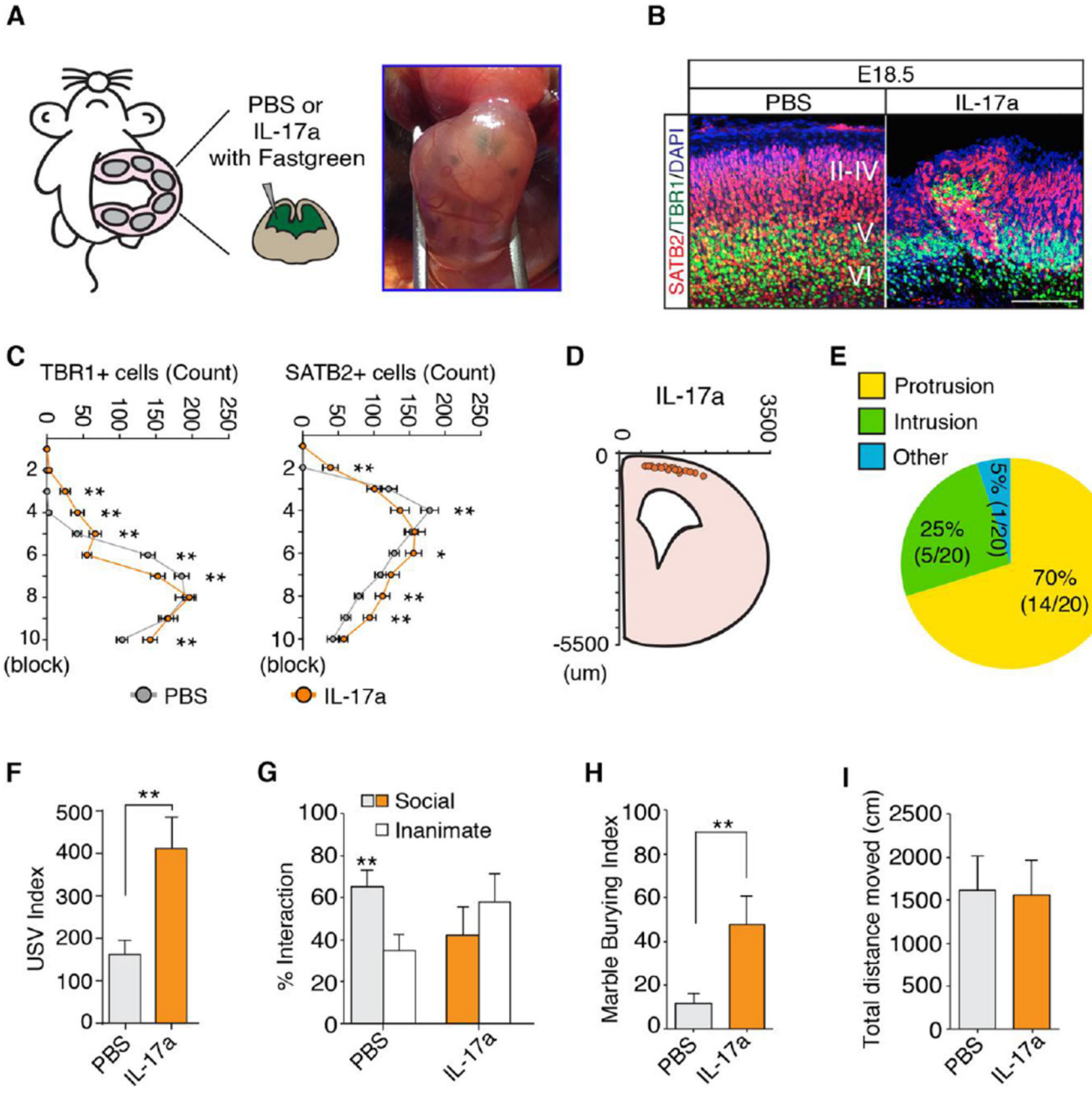

Fig. 5. IL-17a administration to the fetus promotes abnormal cortical development and ASD-like behavioral phenotypes

(**A**) Schematic diagram of the experimental method. Each embryo was injected intraventricularly at E14.5 with PBS or recombinant IL-17a protein mixed with Fastgreen dye. (**B**) SATB2 and TBR1 staining in the cortex of E18.5 male fetal brains treated as in (A). Images are representative of five independent experiments. (**C**) Quantification of TBR1 and SATB2 positive cells in a 300-μm wide ROI corresponding to the region of the cortical plate containing the malformation in E18.5 male fetal brain (n = 20 (PBS), n = 20 (IL-17a)). (**D**) The spatial location of the disorganized cortical patch in E18.5 fetal brain (n = 20 (IL-17a)). (**E**) Percentage of the cortical patches in each category (n = 20 (IL-17a)). (**F**)

Ultrasonic vocalization (USV) assay. The number of pup calls is plotted on the y-axis (n = 15 (PBS), n = 17 (IL-17a); from 5–6 independent dams per treatment). (**G**) Social approach behavior. Graphed as a social preference index (% time spent investigating social or inanimate stimulus out of total object investigation time) (n = 12 (PBS), n = 18 (IL-17a), from 5–6 independent experiments). (**H**) Marble burying behavior. Percentage of the number of buried marbles is plotted on the y-axis (n = 12 (PBS), n = 18 (IL-17a), from 5–6 independent experiments). (**I**) Total distance traveled during social approach test. (C) Two-way ANOVA with Tukey post-hoc tests. (F, H and I) Student's t tests. (G) One-way ANOVA with Tukey post-hoc test. $^{**}P < 0.01$, $^{*}P < 0.05$, and ns; not significant. Graphs show mean ± SEM.

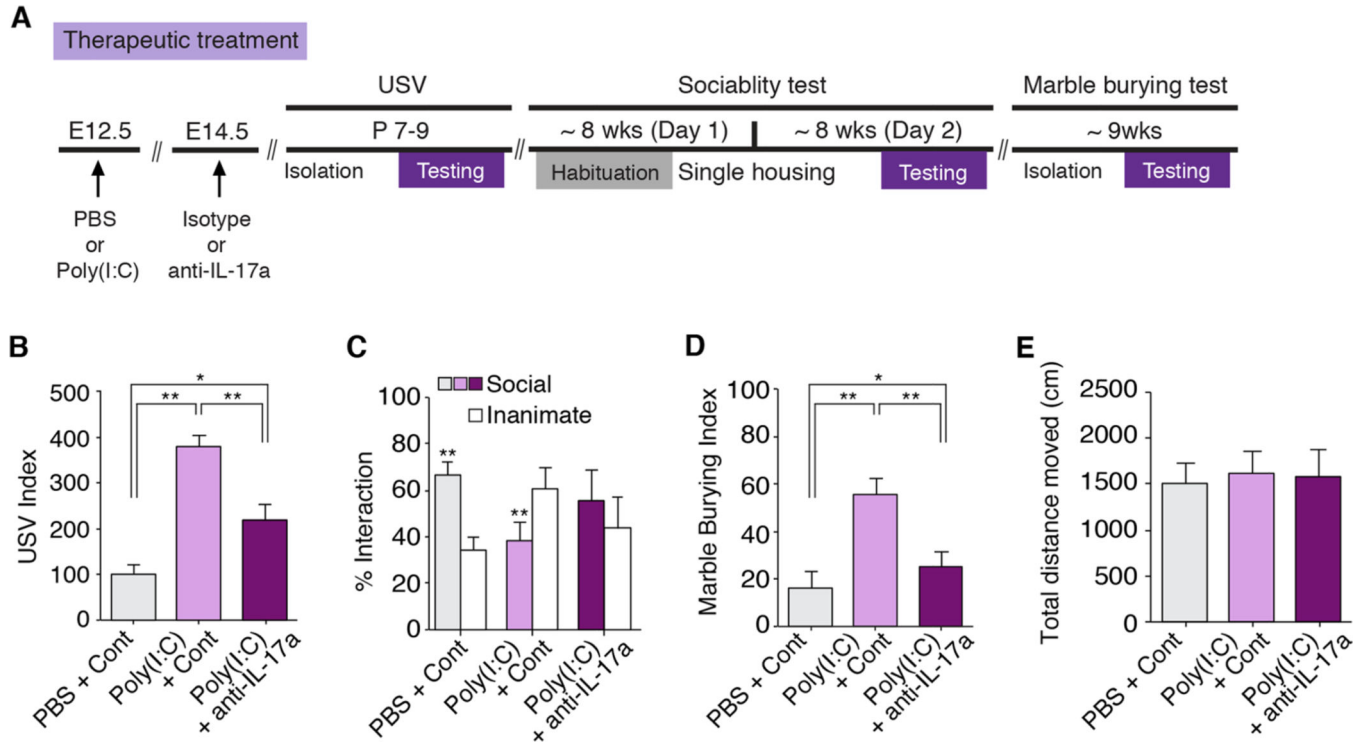

Fig. 6. Therapeutic effects of blocking IL-17a signaling in pregnant dams

(**A**) Schematic diagram of the experimental design. At E12.5, pregnant mothers were injected with PBS or poly(l:C) to induce MIA. Two days later (E14.5), the pregnant mothers were treated with isotype or anti-IL-17a blocking antibodies. At P7~P9, pups were separated from the mothers to measure USV calls. At ~8wks, male offspring were subjected to the social approach test and marble burying test. (**B**) Ultrasonic vocalization (USV) assay. The number of pup calls is plotted on the y-axis (n = 17 (PBS + Cont), n = 17 (Poly(l:C) + Cont), n = 27 (Poly(l:C) + anti-IL-17a; from 3–4 independent dams per treatment). (**C**) Social approach behavior. Graphed as a social preference index (% time spent investigating social or inanimate stimulus out of total object investigation time) (n = 12 (PBS + Cont), n = 10 (Poly(l:C) + Cont), n = 17 (Poly(l:C) + anti-IL-17a; from 3–4 independent dams per treatment). (**D**) Marble burying behavior. Percentage of the number of buried marbles is plotted on the y-axis (n = 12 (PBS + Cont), n = 10 (Poly(l:C) + Cont), n = 17 (Poly(l:C) + anti-IL-17a; from 3–4 independent dams per treatment). (**E**) Total distance traveled during social approach behavior. (B, D and E) One-way ANOVA with Tukey post-hoc tests. (C) Two-way ANOVA with Tukey post-hoc test. $^{**}P < 0.01$ and $^{*}P < 0.05$. Graphs show mean ± SEM.